Gap solitons in nonlinear periodic $\chi^{(2)}$ media

F. C. Moreira,[1] F. Kh. Abdullaev,[1] and V. V. Konotop[1,2]

[1]*Centro de Física Teórica e Computacional, Faculdade de Ciências, Universidade de Lisboa, Avenida Professor Gama Pinto 2,
PT-Lisbon 1649-003, Portugal*
[2]*Departamento de Física, Faculdade de Ciências, Universidade de Lisboa, Campo Grande, Ed. C8, Piso 6, PT-Lisbon 1749-016, Portugal*

The existence, spatial properties, and stability of localized modes in nonlinear quadratic materials with periodically modulated linear refractive index and quadratic nonlinearity (the latter having the zero mean value along the structure) are investigated. The branches of stationary solutions existing in the semi-infinite and three higher gaps are computed. It is shown that modes may possess different symmetries of the fundamental field (i.e., profiles described either by even or odd functions of the transverse coordinate), while requiring the second harmonic to be symmetric. We found that only small-amplitude gap solitons can be stable. The respective modes can bifurcate only from an edge of a total gap when it coincides with the band edge of the linear spectrum of the fundamental field. Moreover, in this case stable modes can be excited with their centers belonging to a slab with either higher or lower refractive index. This simultaneous existence of different stable localized modes can be viewed as a bistability of gap solitons. Examples of the dynamics and excitations of gap solitons are also given.

I. INTRODUCTION

The physics of nonlinear wave processes in periodic media and their optical applications attracted a great deal of attention during recent years [1]. Numerous studies were focused on the band-gap materials with Kerr-type and $\chi^{(2)}$ nonlinearities (for recent reviews see, e.g., [2–5]). In particular, solitons in quadratically nonlinear optical media with shallow and deep periodic modulations of the linear refractive index were investigated in Refs. [6–8], respectively. The structure and stability of spatially localized and periodic stationary field patterns in optical parametric amplifiers and oscillators with a periodically modulated linear refractive index have been addressed in Refs. [9,10]. Such types of materials can be important for the design of optical transistors and switchers [3,11]. Recently, attention has been turned to the study of solitonic structures in materials with periodic modulations of the $\chi^{(2)}$ nonlinearity. In Ref. [12] optical solitons in a two-dimensional quasi-phase-matched geometry involving two concurrent noncollinear quadratic processes have been investigated. It was found that such a system can support a class of localized modes with a large domain of stability. Nonlinear photonic crystals, whose existence in the form of a two-dimensional triangular lattice was suggested in Ref. [13], were experimentally implemented in Ref. [14]. It was shown that the phase-matching resonances are given by a nonlinear Bragg law, what opens possibilities for the generation of a new type of soliton and multiple-beam second-harmonic generation.

There have also been reported studies of structures where both linear and nonlinear modulations of $\chi^{(2)}$ arrays are taken into account. These studies were performed for thin layers with $\chi^{(2)}$ nonlinearity embedded into linear optical media [15]. Such systems can be described by the discrete $\chi^{(2)}$ lattices, where discrete breathers of the different symmetries have been investigated in Ref. [16]. Bright soliton solutions in the second band gap in media with quadratic nonlinearity with a deep Bragg grating are investigated in the work [17] in the framework of the coupled-mode theory approximation. It was shown that only the difference from the shallow grating case [3] is a reduction of the peak intensity of the gap soliton (GS).

In the present work we consider a more general system with simultaneous spatially periodic modulations of linear and nonlinear properties beyond the coupled-mode theory approximation. The nonlinearity is not restricted to thin layers but is considered to have the same spatial distribution as the linear refractive index. More specifically we focus on alternating layers of dielectric materials possessing quadratic nonlinearity and address the localized modes for such systems.

The organization of the paper is as follows. In Sec. II the physical model is described. The asymptotic properties of stationary solutions are studied in Sec. III. In Sec. IV the physical implementation of nonlinear quadratic media periodically modulated parameters is given. A numerical scheme for the solution of the system of equations for $\chi^{(2)}$ media is described in Sec. V A. The GS branches of solutions and their stability are discussed in Secs. V B, V C, and V D. The main results are summarized in the conclusion.

II. THE MODEL

We consider a perfectly matched fundamental field (FF) and the second harmonic (SH) having, respectively, the frequencies ω_1 and $2\omega_1$ and the wave vectors k_1 and $2k_1$. Both waves propagate along the z direction. The medium is considered periodically modulated in the transverse (i.e., the x direction with the spatial period l). Respectively, for the dielectric permittivity we have $\epsilon(x,\omega_j) \equiv \epsilon_j(x) = \epsilon_{0j} + \epsilon_{1j}(x)$, where $\epsilon_{1j}(x) = \epsilon_{1j}(x + l)$ describes the periodic modulation. We also let $\chi_1(x) \equiv \chi^{(2)}(x,\omega_1;2\omega_1,-\omega_1)$ and $\chi_2(x) \equiv \chi^{(2)}(x,2\omega_1;\omega_1,\omega_1)$ with $\chi_j(x) = \chi_j(x + l)$ standing for the second-order susceptibilities. Then in the parabolic approximation the equations governing the field evolution read (see, e.g., [3])

$$2ik_1\frac{\partial E_1}{\partial z} + \frac{\partial^2 E_1}{\partial x^2} + \Delta_1(x)E_1 + 8\frac{\pi\omega_1^2}{c^2}\chi_1(x)\bar{E}_1 E_2 = 0, \quad (1a)$$

$$ik_1\frac{\partial E_2}{\partial z} + \frac{1}{4}\frac{\partial^2 E_2}{\partial x^2} + \Delta_2(x)E_2 + 4\frac{\pi\omega_1^2}{c^2}\chi_2(x)E_1^2 = 0, \quad (1b)$$

where the bar denotes the complex conjugation, $k_j = \omega_1\sqrt{\epsilon_{0j}}/c$, and $\Delta_j(x) = k_1^2\epsilon_{1j}(x)/\epsilon_{01}$. Our consideration will be restricted to lossless media, such that $\chi_2 = \chi_1/2$ is assumed to be satisfied [18].

For the next consideration it is convenient to introduce dimensionless independent $\xi = 2\pi x/l$, $\zeta = 2\pi^2 z/(k_1 l^2)$, and dependent $u_1 = l^2 k_1^2 \chi_{01} E_1/(\pi\epsilon_{01})$ and $u_2 = l^2 k_1^2 \chi_{01} E_2/(\pi\epsilon_{01})$ variables, where $\chi_{01} = \max(\chi_1^{(2)}) - \min(\chi_1^{(2)})$ characterizes the amplitude of modulation of the nonlinear susceptibility for the first harmonic. We also define

$$V_j(\xi) = -\frac{l^2 k_1^2}{4\pi^2\epsilon_{01}}\epsilon_{1j}\left(\frac{\xi l}{2\pi}\right), \quad f(\xi) = \frac{1}{\chi_{01}}\chi_1\left(\frac{\xi l}{2\pi}\right), \quad (2)$$

where $V_{1,2}(\xi) = V_{1,2}(\xi + 2\pi)$ are 2π periodic functions. This leads us to the dimensionless system of equations,

$$i\frac{\partial u_1}{\partial\zeta} + \frac{\partial^2 u_1}{\partial\xi^2} - V_1(\xi)u_1 + 2f(\xi)\bar{u}_1 u_2 = 0, \quad (3a)$$

$$i\frac{\partial u_2}{\partial\zeta} + \frac{1}{2}\frac{\partial^2 u_2}{\partial\xi^2} - 2V_2(\xi)u_2 + f(\xi)u_1^2 = 0. \quad (3b)$$

System (3), where only the linear lattice is present [i.e., where $f(\xi) \equiv$ const.], was considered in Refs. [9,10], while in the presence of only the nonlinear lattice [i.e., at $V_{1,2}(\xi) \equiv$ const.], it was studied in the recent paper [12].

Solutions of Eq. (3) conserve the Hamiltonian,

$$H = \int_{-\infty}^{\infty}\left(\left|\frac{\partial u_1}{\partial\xi}\right|^2 + \frac{1}{2}\left|\frac{\partial u_2}{\partial\xi}\right|^2 + V_1|u_1|^2 \right.$$
$$\left. +2V_2|u_2|^2 - f\bar{u}_1^2 u_2 - fu_1^2\bar{u}_2\right)d\xi, \quad (4)$$

and the total power,

$$P = \int_{-\infty}^{\infty}(|u_1|^2 + 2|u_2|^2)d\xi. \quad (5)$$

III. ASYMPTOTIC PROPERTIES OF STATIONARY SOLUTIONS

We are interested in stationary localized solutions which can be searched in the form,

$$u_j(\xi,\zeta) = w_j(\xi)e^{ijb\zeta} \quad j = 1,2, \quad (6)$$

where $w_j(\xi) \to 0$ at $\xi \to \pm\infty$ and b ($2b$) is the wave-vector detuning of the FF (SH). Following the arguments of Ref. [10], it is possible to prove that for exponentially localized solutions, $w_{1,2}(\xi)$ have constant phases, and thus can be chosen real, and consequently satisfying the equations,

$$-\frac{d^2 w_1}{d\xi^2} + (V_1(\xi) + b)w_1 - 2f(\xi)w_1 w_2 = 0, \quad (7a)$$

$$-\frac{1}{2}\frac{d^2 w_2}{d\xi^2} + 2(V_2(\xi) + b)w_2 - f(\xi)w_1^2 = 0. \quad (7b)$$
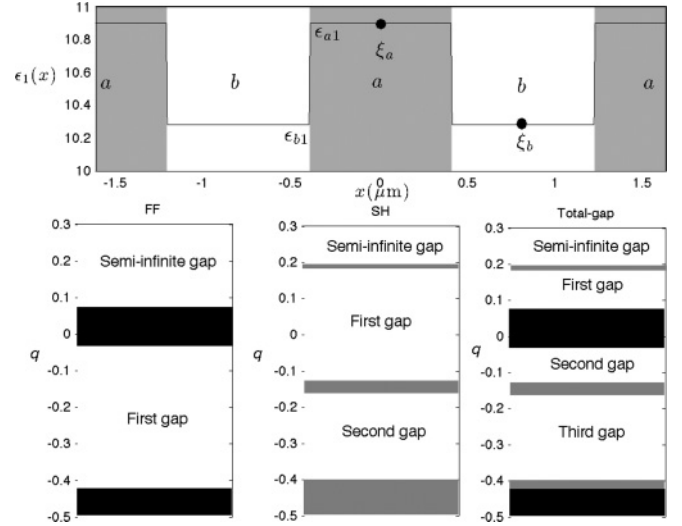

FIG. 1. (Top panel) Schematic presentation of the periodic structure considered in the present paper. The two black circles indicate the coordinates of two symmetry axes (i.e., $\xi_a = 0$ and $\xi_b = \pi$) which are located in the slabs, respectively, with lower (white) and higher (gray) refractive indexes. (Bottom panels) The left panel shows gaps (white) and bands (black) for the FF. Middle panel shows gaps (white) and bands (gray). Right panel shows the resulting total gaps (white) and bands.

It follows from Eq. (7) that the localized stationary solutions obey the integral relation,

$$\int_{-\infty}^{\infty}\left(\frac{dV_1}{d\xi}w_1^2 + 2\frac{dV_2}{d\xi}w_2^2 + \frac{df}{d\xi}w_1^2 w_2\right)d\xi = 0. \quad (8)$$

Below in this work we focus the modulations having well-defined symmetry. More specifically we consider them to be even functions, that is, $V_{1,2}(\xi) = V_{1,2}(-\xi)$ and $f(\xi) = f(-\xi)$ (see Fig. 1 and its description below). Taking into account the symmetry of the periodic medium, we search the solutions of the stationary problem (7) which are either even or odd functions [i.e., which satisfy the relations $w_{1,2}^2(\xi) = w_{1,2}^2(-\xi)$].

Assuming that $w_2(-\xi) = -w_2(\xi)$, we deduce from Eq. (7b) that $f(\xi)w_1^2(\xi)$ is either an odd function, or zero. Since the first possibility is ruled out by the above suppositions about the parity of the nonlinear modulation $f(\xi)$, we conclude that nonlinear localized modes can exist only with an even field of the SH [i.e., with $w_2(\xi) = w_2(-\xi)$]. Meantime Eq. (7a) may support both even and odd profiles of the FF $w_1(\xi)$.

Since $fw_2 \to 0$ at $\xi \to \pm\infty$, the last term in Eq. (7a) decays faster than other ones and thus in the asymptotic region this equation becomes effectively linear. This means that

$$w_1(\xi) \to C_1 A_\pm^{(1)}(\xi), \quad \xi \to \pm\infty, \quad (9)$$

where C_1 is a constant and $A_\pm^{(1)}$ are the solutions of the linear Hill equation,

$$\mathcal{L}^{(1)}A_\pm^{(1)} = -bA_\pm^{(1)}; \quad \mathcal{L}^{(1)} = -\frac{\partial^2}{\partial\xi^2} + V_1(\xi), \quad (10)$$

decaying at $\pm\infty$, respectively. The Floquet theorem assures that these two linearly independent solutions can be expressed in the form,

$$A_{\pm}^{(1)}(\xi) = \phi_1(\pm\xi)e^{\pm\mu_1\xi}. \quad (11)$$

Here $\phi_1(\xi)$ is a 2π-periodic function, and the real Floquet exponent μ_1 is defined by the location of the propagation constant b inside a gap of the spectrum of the operator $\mathcal{L}^{(1)}$ defined in Eq. (10). Denoting the set of the gaps of Eq. (10) by Σ_1, we thus can write the formulated conditions as $b \in \Sigma_1$.

Passing now to the asymptotic of Eq. (7b) we can treat it as an inhomogeneous linear equation for w_2 satisfying the conditions $dw_2(0)/d\xi = 0$ [recall that the mode $w_2(\xi)$ must be necessarily even] and $w_2(\pm\infty) = 0$, with w_1 considered as given. Then the asymptotic behavior of w_2 depends on the relation between the asymptotics of the solution of the linear equation,

$$\mathcal{L}^{(2)}A_{\pm}^{(2)} = -bA_{\pm}^{(2)}, \quad \mathcal{L}^{(2)} = -\frac{1}{4}\frac{\partial^2}{\partial\xi^2} + V_2(\xi), \quad (12)$$

and on the decay of w_1^2 defined by Eq. (11) (i.e., by the exponent $2\mu_1$). In other words, the asymptotic of w_2 depends on the position of a given b with respect to the spectrum of Eq. (12). In the present paper we concentrate only on the cases where b belongs also to a gap of the spectrum of Eq. (12). The set of the respective gaps will be designated as Σ_2 [i.e., we require $b \in \Sigma_2$]. Then the overlap between the two sets of the gap $\Sigma = \Sigma_1 \cap \Sigma_2$ can be referred to as the total gap (see Fig. 1 below), and the situation considered in this paper can be characterized by the condition that b belongs to the total gap (i.e., $b \in \Sigma$).

Since $b \in \Sigma_2$, again using the Floquet theorem one can represent the solutions of Eq. (12) as

$$A_{\pm}^{(2)}(\xi) = \phi_2(\pm\xi)e^{\pm\mu_2\xi}, \quad (13)$$

where $\mu_2 > 0$ and $\phi_2(\xi)$ is a 2π-periodic function.

Now one can distinguish two different cases as follows. In Case 1, the location of b in the total gap is such that $2\mu_1 > \mu_2$ and a solution of the homogeneous equation (12) decays slower than w_1^2, and hence in the asymptotic region $\xi \to \pm\infty$ the behavior of w_2 is defined by the asymptotic (13) (i.e., see Appendix A),

$$w_2(\xi) \to \begin{cases} C_+A_-^{(2)}(\xi) & \text{for} \quad \xi \gg 0, \\ C_+A_+^{(2)}(\xi) & \text{for} \quad \xi \ll 0. \end{cases} \quad (14)$$

In Case 2, where $2\mu_1 < \mu_2$, the asymptotic of Eq. (7b) is given by a particular solution of the inhomogeneous equation (7b). In order to obtain the asymptotic in this case we proceed as it is described in Appendix A, that is, we find that as $\xi \to \infty$,

$$-\frac{W}{2}w_2 \approx C_1^2 \int_\xi^\infty \phi_2(-\xi')(A_-^{(1)})^2 d\xi' [\phi_2(\xi)e^{-\mu_2(\xi'-\xi)} + \phi_2(-\xi)e^{-\mu_2(\xi'+\xi)}] + C_-\phi_2(-\xi). \quad (15)$$

(We notice that the described situation resembles the cases of free-tail and tail-locked cases considered in Ref. [19] for the three-wave gap solitons in quadratic media.)

Thus the specific forms of Eqs. (9), (14), and (15) suggest that two of the parameters C_1 and $C_\pm$ can be used for constructing localized solutions numerically using the shooting method.

IV. A PERIODIC STRUCTURE

In order to proceed with numerical construction of particular solutions, it is necessary to specify the layered structure (i.e., to introduce particular forms of the functions V_j and f). To this end we consider a structure consisting of alternating slabs of two different materials alternating periodically and denoted below by a and b. Respectively, we have

$$V_j(\xi) = \begin{cases} V_{aj} & \text{for} \quad |\xi| < \pi/2, \\ V_{bj} & \text{for} \quad \pi/2 < |\xi| < \pi, \end{cases} \quad (16)$$

where V_{aj} and V_{bj} are constants, and

$$f(\xi) = \begin{cases} f_0 + 1/2 & \text{for} \quad |\xi| < \pi/2, \\ f_0 - 1/2 & \text{for} \quad \pi/2 < |\xi| < \pi. \end{cases} \quad (17)$$

In the numerical studies reported below we use for slabs a and b, respectively, an orientation-patterned gallium arsenide (OP-GaAs) [20] and the alloy $Al_{0.125}Ga_{0.875}As$ [21]. This structure, possessing the required modulation of both dielectric permittivity and of the nonlinear susceptibility, can be fabricated with the combination of techniques such as low-pressure hydride vapor phase epitaxy [20] for the χ_1 modulation and molecular beam epitaxy using Si shadow masks [22]. Both materials are transparent when $k_1^{-1} = 3.18$ μm. Their dielectric constants are $\epsilon_{a1} = \epsilon_{a2} = 10.9$ and $\epsilon_{b1} = \epsilon_{b2} = 10.28$, respectively. Here ϵ_{aj} (ϵ_{bj}) represents the dielectric constant of the a (b) layer on the FF ($j = 1$) or SH ($j = 2$). One has in this case $\epsilon_{01} = 10.59$. We choose the period of the structure to be $l = 1.63$ μm. The modulus of the nonlinear susceptibilities are $\chi_{a1} = 2\chi_{a2} = 94$ pm/V and $\chi_{b1} = 2\chi_{b2} = -94$ pm/V [23]. The constant χ_{aj} (χ_{bj}) is the nonlinear susceptibility in the a (b) layer at the FF ($j = 1$) or SH ($j = 2$). The axis of the GaAs and $Al_{0.125}Ga_{0.875}As$ are inverted in respect to one another, such that the second-order susceptibility changes sign from layer to layer. Thus we have $\chi_{01} = 188$ pm/V. This particular structure corresponds to $f_0 = 0$, $V_{a1} = V_{a2} = 0.31$, and $V_{b1} = V_{b2} = -0.31$ in dimensionless form and is schematically illustrated in Fig. 1.

We notice that the introduced structure has two symmetry axes passing through the centers of the layers of each type (i.e., through the points $\xi_a = 0$ and $\xi_b = \pi$).

V. GAP SOLITONS

A. On numerical procedure

In order to obtain the localized modes in this paper we use a shooting method in which shooting starts at some point, say ξ_f, far enough from the origin where the asymptotic expressions (9), (14), and (15) can be used. The shooting parameters are C_1 and C_+ for the $2\mu_1 > \mu_2$ case, and C_1 and C_- for the $2\mu_1 < \mu_2$. In our implementation, we fix C_1 and scan either C_+ or C_- in order to satisfy $w_2'(0) = 0$ [recall that the component $w_2(\xi)$ is an even function]. This procedure is repeated for different C_1 until $w_1'(0) = 0$ (for even modes) or $w_1(0) = 0$ (for odd modes) is satisfied.

For given shooting parameters the integration in the interval $0 \leqslant \xi \leqslant \xi_f$ is done by alternating the two steps as follows. As the first step we integrate (7a) using the Runge-Kutta method and assuming $w_2(\xi)$ to be constant in order to find $w_1(\xi - \delta)$, where δ is a small interval (we used $\delta = 0.01$). As the second step, in Eq. (7b) we use the linear interpolation of w_1 in the interval δ to find $w_2(\xi - \delta)$. Then the procedure is repeated until ξ reaches 0. In this way the sooting method allows us to obtain solutions with the precision of order of 10^{-4}. In order to increase the accuracy further we employed the solution obtained using the shooting method as a seed for a Newton-Raphson solver. The final accuracy of the obtained solutions was of the order of 10^{-10}.

B. Bifurcation of branches from continuum spectrum

Since we are interested in gap solitons belonging to one of the total gaps it becomes relevant whether such gaps have edges coinciding with edges of the FF bands or with edges of the SH bands. For the layered structure at hand one observes from Fig. 1 that the total semi-infinite gap is limited by the upper branch of the SH, while the first highest total gap has the upper boundary from the band spectrum of the SH and the lower boundary coinciding with the boundary for the semi-infinite

gap for the FF. As we will see below these facts have direct implications on the existence of small-amplitude gap solitons.

In order to clarify this last point we now turn to the analysis of the small-amplitude limit, and more specifically we address the possibility of having families of the gap solitons bifurcating from the continuum spectrum (i.e., from the linear Bloch states). In the general analysis performed below we exclude the possibility of two coinciding edges of bands of the FF and SH (what in particular corresponds to the medium shown in Fig. 1). Then from Eq. (7) we deduce the conclusion that no branches can bifurcate from the edge of the total gap, which is originated by the spectrum of the SH. Indeed, assuming the opposite we should have w_2 tending to zero [i.e., to the linear spectrum of the problem (12)], while $w_1(\xi)$ for the respective propagation constant, having nonzero detuning to a gap of the spectrum of the linear problem (12), should have zero limit. This obviously contradicts to Eq. (7b), which in the described case should have the first two terms much smaller than the last one.

In other words, a branch of solutions (if any) can bifurcate only from the boundary of the total gap coinciding with boundary of a gap of the FF. This is, however, is only a necessary condition for the existence of a bifurcating branch but not yet enough one. The second necessary condition comes from the requirement of the instability of the Bloch states
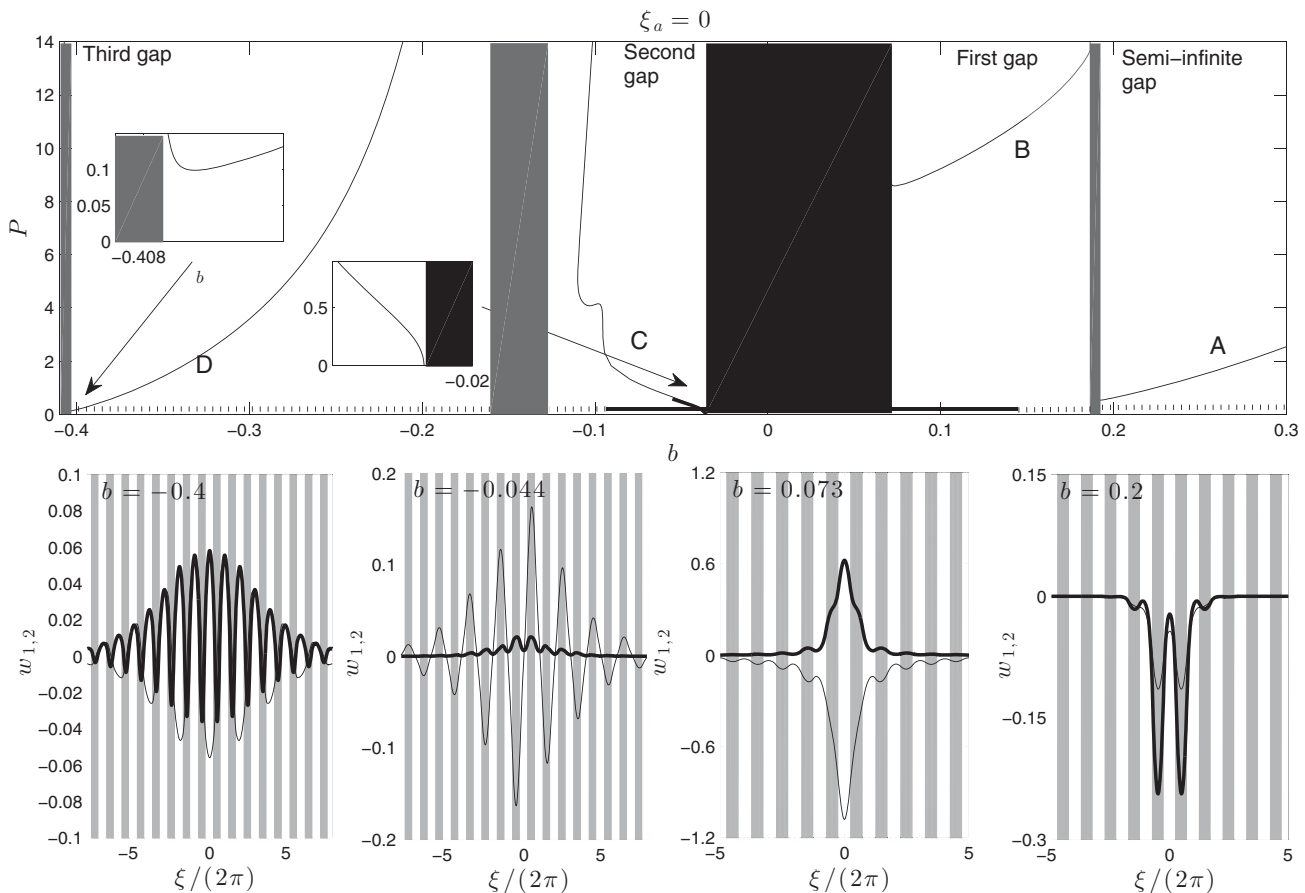

FIG. 2. (Top panel) The lowest branches of the solutions centered at $\xi_a = 0$ which belong to the semi-infinite gap and to the three highest total gaps of the spectrum. Thick (thin) lines denote stable (unstable) solutions. Gray and black bars represent FF and SH bands, respectively. In the abscissa axis we use the thick (dotted) lines to indicate the range of the propagation constant where $2\mu_1 < \mu_2$ ($2\mu_1 > \mu_2$). (Bottom panels) Examples of gap solitons for the branch of each total gap starting from the semi-infinite total gap on the right. Thick (thin) lines represent w_2 (w_1).

bordering the respective gap edge. This issue can be addressed within the framework of the multiple scale expansion [24]. Indeed, when a branch bifurcates from a gap edge of the FF, then w_1 is small. If at the same time w_2 is not small, since in this case it does not border any gap edge of the SH, we again arrive at the contradiction because now Eq. (7b) in the leading order becomes linear. This means that no small-amplitude limit with $w_1 = o(w_2)$ is possible. This is what would happen in the case $2\mu_1 > \mu_2$. In the case $2\mu_1 < \mu_2$, however, one can require w_2 to be much smaller than w_1. Then Eq. (7b) may have a small-amplitude solution which obeys the scaling $w_2 \sim w_1^2$. Thus to find (approximately) such a solution we have to explore the expansions in the form,

$$u_1 = \kappa u_1^{(1)} + \kappa^2 u_1^{(2)} + \cdots, \quad u_2 = \kappa^2 u_2^{(2)} + \cdots, \quad (18)$$

where $\kappa \ll 1$ is a formal small parameter and $\xi_j = \kappa^j \xi$ and $\zeta_j = \kappa^j \zeta$ are the scale variables, regarded as independent. In the vicinity of a given band edge (let it be the α_0th band) the leading order of the solution is searched in the form,

$$u_1^{(1)}(\xi_0, \zeta_0) = U_1(\xi_1, \zeta_2) \phi_{\alpha_0 q_0}^{(1)}(\xi_0) e^{i b_{\alpha_0 q_0}^{(1)} \zeta_0} + \text{c.c.}, \quad (19)$$

where $U_1(\xi_1, \zeta_2)$ is a slowly varying envelope. The further steps are standard, and therefore we only briefly outline them

in Appendix B. The resulting equation for the small amplitude reads

$$i \frac{\partial U}{\partial Z} = -\frac{\partial^2 U}{\partial X^2} + \sigma |U|^2 U, \quad (20)$$

where $\sigma = \pm 1$ and is defined in Eq. (B7) in Appendix B. Thus the second condition which must be satisfied for existence of a solitonic branch bifurcating from a gap edge is that $\sigma < 0$.

C. Branches of solutions

Turning to the discussion of the branches of the solution we notice that the symmetry of the structure implies the existence of two different families of solutions, corresponding to two different symmetry axes of the structure (see Fig. 1). We address the solitons which are centered either in a slab with lower refractive index, that is, at $\xi_a = 0$ (shown in Fig. 2) or in an optically more dense slab, that is, in the point $\xi_b = \pi$ (see Fig. 3).

As the first step, using (B6) and (B7) we computed σ for all edges of the total gaps, coinciding with the gap edges of the FF. It turns out that for the structure at hand only the edge defined by $b_{0,1/2}^{(1)} \approx -0.3573$ (i.e., at the boundary of the Brillouin zone, that is, corresponding to a finite total gap) has $\sigma = -1$. Hence this is the only edge where a branch of the gap soliton solutions can bifurcate from the linear spectrum. This is precisely what the curves C, bifurcating from the upper
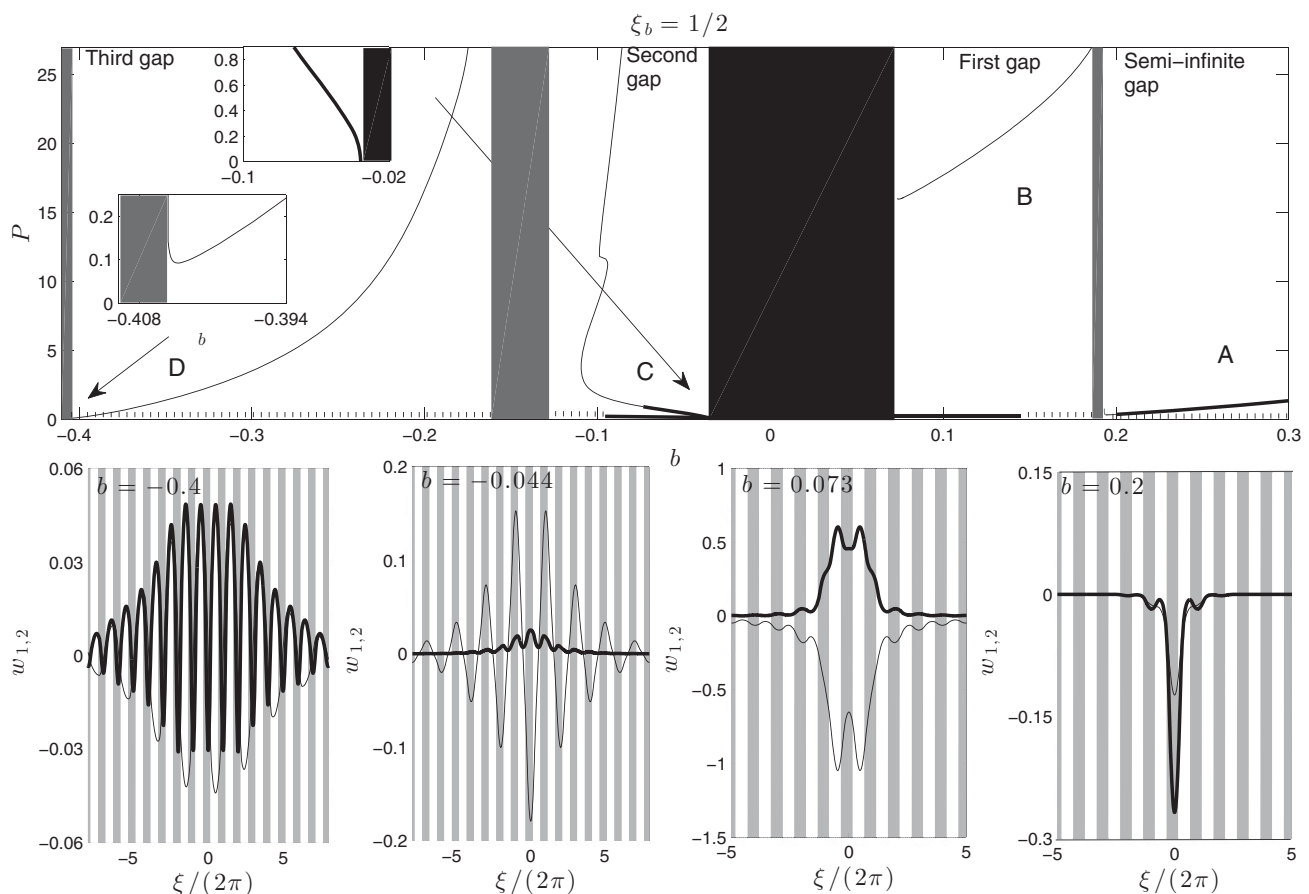

FIG. 3. The same as in Fig. 2 but for the branches of solitons centered at $\xi_b = \pi$. Notice that here we introduced the π shift in the coordinate ξ (with respect to the ξ axis shown in Fig. 1) in order to place the soliton centers in the origin.

edge of the second total gap, in Figs. 2 and 3 show. In the low intensity limit, the SH appears only as a small perturbation to the FF, what one can also observe in the second lower panels in Fig. 2 ($b = -0.044$) and 3 ($b = -0.48$). The comparison of these two figures reveals the first interesting phenomenon: The symmetry of the fundamental field is changed depending on the center location.

Since we are in the small-amplitude limit, this change of the symmetry is understandable from the requirement for the light to concentrate in the waveguides with higher refractive index (the gray strips). This also gives the physical understanding for the observed stability of the modes. This is another important property, which can be interpreted as *bistability of gap solitons*, which manifests itself in existing two different branches of the solutions bifurcating from the same gap edge. Both branches C have overlapping intervals of the stability of the solutions.

It is worth mentioning an example of the first total gap, where at the edge where $b_{0,0}^{(1)} = 0.0724$ (it coincides with the band edge of the FF) one has $\sigma = 1$ while the upper edge coincides with the band edge of the SH. Therefore the lowest branch of the solutions (see curves B in Figs. 2 and 3) does not approach zero at any of the gap edges: At the lower edge because the NLS equation (20) does not possess bright solutions when $\sigma = 1$, while at the upper edge because the branch borders the SH edge.

In general we observe that Eq. (20), obtained by multiple-scale expansion, gives the result which is in good agreement with the corresponding numerical solution of the system (7). This is illustrated in Fig. 4.

Localized modes may have the field concentrated in the slabs with lower refractive index. This is observed in the third and first total gaps if the mode is centered in the waveguide with lower refractive index (respectively, the first and third lower panels in Figs. 2 and 3). As expected, such modes are unstable.

Probably the most important distinction of the modes centered in different domains is that while in both cases one can find branches of solutions in the semi-infinite gap, only the "one-hump" mode having its maximum in a slab with larger refractive index (the lower panel with $b = 0.2$ in Fig. 3) appears to be stable if the propagation constant exceeds some
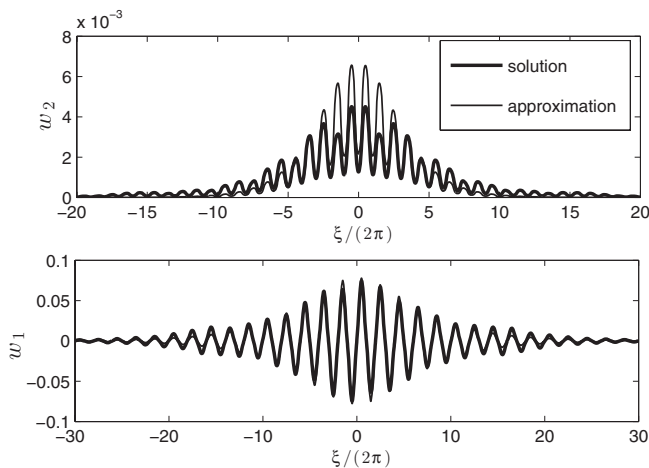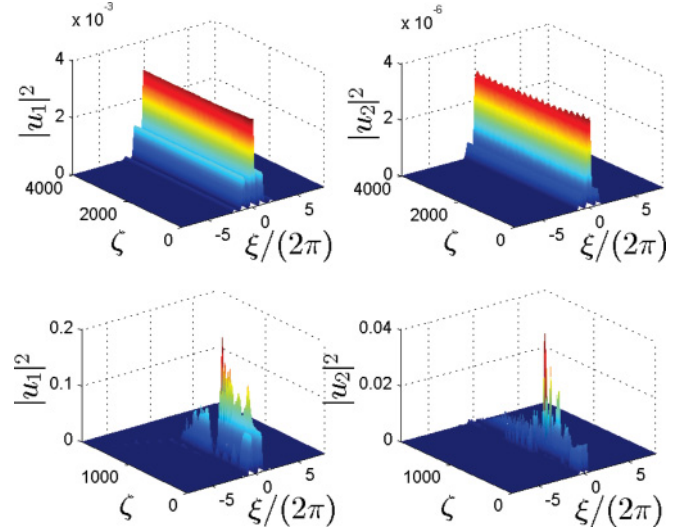

FIG. 5. (Color online) (Top panels) Stable propagation of the soliton centered in $\xi_a = 0$ and having $b = -0.05$ (curve C in Fig. 2), integrated up to $\zeta = 4000$. (Bottom panels) Unstable propagation of a solution centered at $\xi_a = 0$ and having $b = -0.1$ (curve C in Fig. 2), integrated up to $\zeta = 2000$. In all simulations the input beam was perturbed by noise of the order of 10% of the soliton amplitude.

critical value (c.f. A, branches in the semi-infinite bands shown in Figs. 2 and 3).

In the semi-infinite and third total gaps (branches A and D in Figs. 2 and 3) both edges are from the SH gap. As we previously explained, the small-amplitude limit is not possible in this case.

D. On dynamics of gap solitons

The stability of the modes discussed above has been checked both by the analysis of the linear stability and by the direct propagation. The results of this last test are illustrated in Fig. 5 where we show the propagation of a randomly perturbed
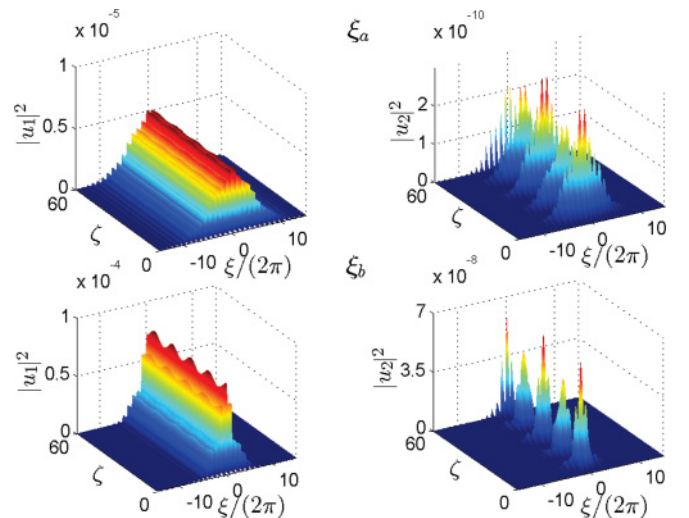

FIG. 4. Panels show comparison of approximated model with numerical solution with $\xi_a = 0$ and $b = -0.038$.

FIG. 6. (Color online) Top (bottom) panel shows evolution of the initial condition $u_1(\xi,0) = w_1(\xi)$ and $u_2(\xi,0) = 0$, where $w_1(\xi)$ is a solution of Eq. (7) with $b = -0.038$, corresponding to branch C and centered at ξ_a (ξ_b).

input beam corresponding to stable and unstable parts of the same branch of the solution.

Next we concentrate on the possibilities of the exciting stationary gap solitons by an input field consisting of only FF. The respective dynamics, obtained by the direct numerical integration of Eq. (3), is shown in Fig. 6 where we used the initial conditions of the form $u_1(\xi,0) = w_1(\xi)$ and $u_2(\xi,0) = 0$. Dynamics of FF and SH is shown in the left and right panels, respectively. Both examples illustrate persisting localized solutions with almost all energy localized in the fundamental mode, and periodic exchange of a relatively small amount of energy between the modes. The energy oscillations have a period ≈ 14 for both examples.

VI. CONCLUSIONS

To conclude, we have investigated the existence, spatial properties, and stability of localized modes in nonlinear quadratic materials with a periodically modulated linear refractive index and quadratic nonlinearity. An important assumption about the structure was that its quadratic non-linearity averaged over the transverse direction is zero. We considered in detail asymptotic properties of the solutions which revealed two different types of behavior, corresponding to dominating asymptotic of either the fundamental field or the second harmonic. These asymptotics were used for the shooting method, using which we computed the branches of the stationary solutions existing in the semi-infinite and three higher gaps. We have shown that modes may possess different symmetries (i.e., have profiles described either by even or by odd functions) of the fundamental field, but require the second harmonic to be symmetric.

The modes may have the field energy to be concentrated either in slabs with a higher or with a lower refractive index. However, only the former ones turn out to be stable. Moreover, we found that only small-amplitude gap solitons are stable. Such modes can bifurcate only from the edge of the total gap (i.e., the domain of the propagation constant which in the linear limit is forbidden for both fundamental and second harmonics) when it coincides with the band edge of the first harmonic. The stable modes can be excited with centers belonging either to a slab with the higher refractive index or a slab with the lower one. This simultaneous existence of different stable modes localized can be viewed as a bistability of gap solitons. Examples of the dynamics and excitations of gap solitons by applying only the fundamental field are also given. In this case the propagation of persisting localized beams is accompanied by the energy exchange between the first and second harmonics.

Finally, we mention quite a different physical system where similar kinds of gap solitons may be observable. It is an atomic-molecular Bose-Einstein condensate loaded in optical lattices [25], where the modulation of "quadratic nonlinearity" is performed by manipulating the atomic-molecule scattering length in space using the Feshbach resonance technique [26].

APPENDIX A: DERIVATION OF EQS. (14) AND (15)

Using the Green function,

$$G(\xi,\xi') = \begin{cases} A_+^{(2)}(\xi)A_-^{(2)}(\xi') & \text{for} \quad \xi < \xi', \\ A_+^{(2)}(\xi')A_-^{(2)}(\xi) & \text{for} \quad \xi > \xi', \end{cases} \quad \text{(A1)}$$

Eq. (7b) can be rewritten in the integral form,

$$w_2(\xi) = -\frac{2}{W} \int_{-\infty}^{\infty} G(\xi,\xi') f(\xi') w_1^2(\xi') d\xi', \quad \text{(A2)}$$

where $W = A_-^{(2)} dA_+^{(2)}/d\xi - A_+^{(2)} dA_-^{(2)}/d\xi$ is the Wronskian.

One can distinguish two asymptotic regimes in Eq. (A2). In the first case, when $2\mu_1 > \mu_2$, from Eq. (9) we conclude that the integral,

$$C_+ = \int_0^{\infty} (A_+^{(2)} + A_-^{(2)}) f w_1^2 d\xi', \quad \text{(A3)}$$

exists. This allows us to write (A2) as

$$-\frac{W}{2} w_2 = A_+^{(2)}(\xi) \int_{\xi}^{\infty} A_-^{(2)} f w_1^2 d\xi'$$
$$- A_-^{(2)}(\xi) \int_{\xi}^{\infty} A_+^{(2)} f w_1^2 d\xi' + C_+ A_-^{(2)}. \quad \text{(A4)}$$

Both terms containing integrals in this expression decay faster than $C_+ A_-^{(2)}$ as $\xi \to \infty$. Thus the total solution decays with exponent μ_2.

The second case corresponds to $2\mu_1 < \mu_2$. For some $\xi = \xi_f$ far enough from the origin, one can approximate $w_1(\xi_f) \approx C_1 A_-^{(1)}(\xi_f)$ and obtain (15), where

$$C_- = \int_{-\xi_f}^{\xi_f} \phi_2(\xi) e^{-\mu_2(\xi_f - \xi)} f(\xi) w_1^2(\xi) d\xi. \quad \text{(A5)}$$

APPENDIX B: DERIVATION OF EQ. (20)

Let us notice that the wave vector can be at the center ($q_0 = 0$) or at the edge($q_0 = 1/2$) of the first Brillouin zone and introduce the notations $\phi_{\alpha q}^{(j)}(\xi_0)$ and $b_{\alpha q}^{(j)}(j = 1,2)$ for the orthonormal Bloch states and the respective eigenvalues of the operator $\mathcal{L}^{(j)}$ ($j = 1,2$): $\mathcal{L}^{(j)}\phi_{\alpha q}^{(j)}(\xi) = -b_{\alpha q}^{(j)}\phi_{\alpha q}^{(j)}(\xi_0)$. It follows from the Floquet theorem that $\phi_{\alpha q}^{(1)} = u_{\alpha q}^{(1)}(\xi_0)e^{iq\xi}$ and $u_{\alpha q}^{(1)}(\xi + 2\pi) = u_{\alpha q}^{(1)}(\xi_0)$.

For the sake of simplicity and approaching the statement of the problem closer to the reality we consider a finite structure, having a large length $L = 2N\pi$ ($N \gg 1$ is an uinteger) and impose the cyclic boundary conditions in the interval $0 \leqslant \xi_0 \leqslant L$, where $L = 2N\pi$ and N is a large integer.

Substituting (18) and the scaled variables in Eq. (3) we obtain in the first order of κ $i \frac{\partial u_1^{(1)}}{\partial \zeta_0} - \mathcal{L}^{(1)} u_1^{(1)} = 0$. This equation is solved by the ansatz (19).

In the second order of κ we have

$$i \frac{\partial u_1^{(2)}}{\partial \zeta_0} - \mathcal{L}^{(1)} u_1^{(2)} = -2 \frac{\partial \phi_{\alpha_0 q_0}^{(1)}}{\partial \xi_0} \frac{\partial U_1}{\partial \xi_1} - i \phi_{\alpha_0 q_0}^{(1)} \frac{\partial U_1}{\partial \zeta_1}. \quad \text{(B1)}$$

The solution $u_1^{(2)}$ is searched in the form,

$$u_1^{(2)} = \sum_{\alpha \neq \alpha_0} b_\alpha \phi_\alpha^{(1)} e^{i g_{\alpha_0}^{(1)} \zeta_0} + \text{c.c.} \quad \text{(B2)}$$

In above $\phi_\alpha^{(1)} = \phi_{\alpha q_0}^{(1)}$. Substituting (B2) in Eq. (B1) and projecting in all Bloch functions it is possible to obtain

$$g_\alpha = 2 \frac{\Gamma_\alpha^{(1)}}{b_{\alpha_0}^{(1)} - b_\alpha^{(1)}} \frac{\partial U_1}{\partial \xi_1}, \quad \Gamma_\alpha^{(1)} = \int_0^{2\pi} u_\alpha^{(1)} \frac{\partial u_{\alpha_0}^{(1)}}{\partial \xi_0} d\xi_0. \quad \text{(B3)}$$

Now we investigate the κ^2-order equation of the SH,

$$\frac{1}{2} i \frac{\partial u_2^{(2)}}{\partial \zeta_0} - \mathcal{L}^{(2)} u_2^{(2)} = -\frac{1}{2} f(\xi_0) \left(\phi_{\alpha_0}^{(1)} \right)^2 U_1^2. \quad \text{(B4)}$$

We look for solutions in the form,

$$u_2^{(2)} = \sum_{(\alpha, q)} c_{\alpha q}(\xi_1, \zeta_2) \phi_{\alpha q}^{(2)} e^{2i b_{\alpha_0}^{(1)} \zeta_0} + \text{c.c.} \quad \text{(B5)}$$

The expansion (B5) is valid since we excluded a possibility for $b_{\alpha q}^{(2)}$ to approach $b_{\alpha_0}^{(1)}$ (see Fig. 1). Next we substitute (B5)

in Eq. (B4) and projecting on $\phi_{\alpha q}^{(2)}$ obtain

$$c_\alpha = \frac{\Gamma_\alpha^{(2)} U_1^2}{2 \left(b_{\alpha_0}^{(1)} - b_\alpha^{(2)} \right)}, \quad \Gamma_\alpha^{(2)} = \int_0^{2\pi} u_\alpha^{(2)} f(\xi_0) \left(u_{\alpha_0}^{(1)} \right)^2 d\xi_0.$$

Here we took into account that only wave vectors $q = 2q_0$ give nonzero terms in the expansion. Since $2q_0$ is either 0 or a vector of the reciprocal lattice, only the functions $\phi_{\alpha 0}^{(2)}$ enter in Eq. (B6).

Notice that $f(\xi_0)(u_{\alpha_0}^{(1)})^2$ is always even. This means that $c_\alpha = 0$ if $u_\alpha^{(2)}$ is odd. Finally we write the equation of order κ^3,

$$i \frac{\partial u_1^{(3)}}{\partial \zeta_0} - \mathcal{L}^{(1)} u_1^{(3)} = -i \frac{\partial u_1^{(1)}}{\partial \zeta_2} - i \frac{\partial u_1^{(2)}}{\partial \zeta_1} - \frac{\partial^2 u_1^{(1)}}{\partial \xi_1^2}$$
$$- 2 \frac{\partial}{\partial \xi_0} \frac{\partial}{\partial \xi_1} u_1^{(2)} - 2 f(\xi) \overline{u_1^{(1)}} u_2^{(2)}.$$

Projecting this equation on $\phi_{\alpha_0}^{(1)}$ and rescaling $U = \sqrt{|F_1/D|} U_1$ where

$$D = 1 + 2 \sum_{\alpha \neq \alpha_0} \frac{\left| \Gamma_\alpha^{(1)} \right|^2}{b_{\alpha_0}^{(1)} - b_\alpha^{(1)}}, \quad F_1 = \sum_\alpha \frac{\left| \Gamma_\alpha^{(2)} \right|^2}{b_\alpha^{(2)} - b_{\alpha_0}^{(1)}}, \quad \text{(B6)}$$

$Z = D\zeta_2$ and $X = \xi_1$ we arrive at Eq. (20) where

$$\sigma = \text{sign}(FD). \quad \text{(B7)}$$

Notice that the function $f(\xi)$ plays a fundamental role in the definition of the sign of F while D is fixed by linear potential $V_1(\xi)$.

[1] Y. V. Kartashov, V. A. Vysloukh, and L. Torner, Prog. Opt. **52**, 63 (2009); Y. V. Kartashov, B. A. Malomed, and L. Torner, Rev. Mod. Phys. **83**, 247 (2011).

[2] S. Trillo, C. Conti, G. Assanto, and A. V. Buryak, Chaos **10**, 590 (2000).

[3] A. V. Buryak, P. D. Trapani, D. V. Skryabin, and S. Trillo, Phys. Rep. **370**, 63 (2002).

[4] B. A. Aceves, Chaos **10**, 584 (2000).

[5] F. Lederer, G. I. Stegeman, D. N. Christodoulides, G. Assanto, M. Segev, and Y. Silberberg, Phys. Rep. **463**, 1 (2008).

[6] H. He and P. D. Drummond, Phys. Rev. Lett. **78**, 4311 (1997).

[7] T. Peschel, U. Peschel, F. Lederer, and B. A. Malomed, Phys. Rev. E **55**, 4730 (1997); A. Arraf and C. Martijnde Sterke, *ibid.* **58**, 7951 (1998).

[8] Z. Xu, Y. V. Kartashov, L.-C. Crasovan, D. Mihalache, and L. Torner, Phys. Rev. E **71**, 016616 (2005).

[9] Y. V. Kartashov, V. A. Vysloukh, and L. Torner, Opt. Lett. **29**, 1117 (2004); **29**, 1399 (2004).

[10] V. A. Brazhnyi, V. V. Konotop, S. Coulibaly, and M. Taki, Chaos **17**, 037111 (2007).

[11] M. Scalora, J. P. Dowling, C. M. Bowden, and M. J. Bloemer, Phys. Rev. Lett. **73**, 1368 (1994).

[12] A. Pasquazi and G. Assanto, Phys. Rev. A **80**, 021801(R) (2009).

[13] V. Berger, Phys. Rev. Lett. **81**, 4136 (1998).

[14] K. Gallo, A. Pasquazi, S. Stivala, and G. Assanto, Phys. Rev. Lett. **100**, 053901 (2008).

[15] A. A. Sukhorukov, Y. S. Kivshar, O. Bang, and C. M. Soukoulis, Phys. Rev. E **63**, 016615 (2000).

[16] O. Bang, P. L. Christiansen, and C. B. Clausen, Phys. Rev. E **56**, 7257 (1997).

[17] A. Arraf, C. M. de Sterke, and H. He, Phys. Rev. E **63**, 026611 (2001).

[18] Y. R. Shen, *The Principles of Nonlinear Optics* (Wiley, New York, 1984).

[19] W. C. K. Mak, B. A. Malomed, and P. L. Chu, Phys. Rev. E **58**, 6708 (1998).

[20] D. F. Bliss, C. Lynch, D. Weyburne, K. O'Hearn, and J. S. Bailey, J. Crystal Growth **287**, 673 (2006).

[21] S. Adachi, *GaAs and Related Materials: Bulk Semiconducting and Superlattice Properties* (World Scientific, Singapore, 1994).

[22] W. T. Tsang and M. Ilegems, Appl. Phys. Lett. **31**, 301 (2009).

[23] T. Skauli, K. L. Vodopyanov, T. J. Pinguet, A. Schober, O. Levi, L. A. Eyres, M. M. Fejer, and J. S. Harris, Opt. Lett. **27**, 628 (2002); J. Appl. Phys. **74**, 596 (1993).

[24] C. M. de Sterke and J. E. Sipe, Phys. Rev. A **38**, 5149 (1988).

[25] F. Kh. Abdullaev and V. V. Konotop, Phys. Rev. A **68**, 013605 (2003).

[26] R. Yamazaki, S. Taie, S. Sugawa, and Y. Takahashi, Phys. Rev. Lett. **105**, 050405 (2010).